Taylor & Francis
Taylor & Francis Group

REPORT

OPEN ACCESS | Check for updates

Beyond bispecificity: Controlled Fab arm exchange for the generation of antibodies with multiple specificities

Desislava Yanakieva[a,b], Lukas Pekar[b], Andreas Evers[b], Markus Fleischer[c], Stephan Keller[c], Dirk Mueller-Pompalla[c], Lars Toleikis[b], Harald Kolmar[a], Stefan Zielonka[b], and Simon Krah[b]

aInstitute for Organic Chemistry and Biochemistry, Technische Universität Darmstadt, Darmstadt, Germany; bProtein Engineering and Antibody Technologies, Protein Engineering and Antibody Technologies, Merck Healthcare KGaA, Darmstadt, Germany; cProtein and Cell Sciences, Merck Healthcare KGaA, Darmstadt, Germany

ABSTRACT

Controlled Fab arm exchange (cFAE) has proven to be a generic and versatile technology for the efficient generation of IgG-like bispecific antibodies (DuoBodies or DBs), with several in clinical development and one product, amivantamab, approved by the Food and Drug Administration. In this study, we expand the cFAE-toolbox by incorporating VHH-modules at the C-termini of DB-IgGs, termed DB-VHHs. This approach enables the combinatorial generation of tri- and tetraspecific molecules with flexible valencies in a straightforward fashion. Using cFAE, a variety of multispecific molecules was produced and assessed for manufacturability and physicochemical characteristics. In addition, we were able to generate DB-VHHs that efficiently triggered natural killer cell mediated lysis of tumor cells, demonstrating the utility of this format for potential therapeutic applications.

Introduction

The immune system continuously combats adversaries such as malignant cells and pathogens that are potentially harmful to the human body. While innate immunity mainly interacts with highly conserved structures via more promiscuous and less specific receptors, the receptors of adaptive immunity are of high specificity and affinity.[1] Key players of the adaptive immune system are antibodies, produced by activated B cells. Antibodies can recognize a variety of foreign substances (antigens) and lead to pathogen degradation, e.g., via immune cell activation.[2] Technologies to generate tailored monoclonal antibodies (mAbs), initially via mouse immunization and hybridoma-technology,[3,4] have been used for decades to develop antibody therapeutics. In 2021, the 100th mAb product was approved by the Food and Drug Administration (FDA), manifesting antibodies as one of the major modalities in drug discovery.[5]

Besides classical mAbs, bispecific antibodies (bsAbs) promise to be more efficacious in certain therapeutic settings since they can modulate more than one disease mediator.[6,7] However, the generation of these antibodies requires extensive engineering. In general, bispecifics can be produced as non-IgG and IgG-like molecules.[8] While non-IgG bsAbs lack an Fc portion and mainly consist of only one polypeptide chain, IgG-like antibodies are Fc-bearing molecules.[9] The latter can be equipped with beneficial Fc-functionalities such as long in vivo half-life and immune cell activation via Fc receptors, but different polypeptide chains need to assemble correctly during the manufacturing process.[10,11] Several technologies were developed that force heavy chain heterodimerization, including knobs-into-holes, DEKK mutations and strand-exchanged engineered domains (SEEDs).[12–14] Still, the expression of a heavy chain heterodimerized antibody requires further engineering to ensure correct light chain pairing. In its simplest form, this can be mediated by single-chain variable fragment grafting of one paratope, which, however, often comes with substantial stability issues and diminished affinities.[15] Other technologies make use of domain swapping or electrostatic steering.[11] In all, many alterations need to be incorporated into an antibody sequence to obtain a bispecific molecule with correctly paired heavy and light chains. These bsAbs are often challenging to produce and may be immunogenic when used as drugs in humans.[16]

Another way to generate bsAbs is inspired by a natural process of the immune repertoire, called Fab arm exchange (FAE). IgG4 molecules undergo FAE, which results in randomly paired bsAbs in vivo. Compared to other subclasses, these antibodies are monovalent for a respective antigen, which reduces their ability to crosslink antigens and form immune complexes. It is believed that a competition of such IgG4 molecules with antibodies from other subclasses attenuates inflammatory reactions.[17,18] FAE can also be used to generate bsAbs in vitro. In a screening approach, Labrijn et al.[19] incorporated IgG4 mutations in IgG1 CH3 to find residues that destabilize the IgG homodimer and promote heterodimer formation after incubation of single-point mutated antibodies under reducing conditions. One pair of these matching CH3 mutations was identified as F405L in one and K409R in the other antibody. The process referred to as "controlled FAE" (cFAE) leads to IgG-like

CONTACT Stefan Zielonka; Simon Krah ✉ stefan.zielonka@merckgroup.com; simon.krah@merckgroup.com ● Protein Engineering and Antibody Technologies, Merck Healthcare KGaA, Darmstadt, Germany
Supplemental data for this article can be accessed on the publisher's website.

bsAbs, wherein no light chain mispairing occurs and only two mutations are introduced into the pair of antibody CH3 domains.[20] Compared to conventional methods for bsAb generation, cFAE may lead to bispecifics with less immunogenicity.[21] In terms of manufacturability, cFAE might be more modular, but it requires the development of good manufacturing practice-compliant processes for two independent antibodies and another process step for antibody recombination.

Developed by Genmab, cFAE is used to generate bsAbs termed DuoBodies (DBs). Today, several DBs are in clinical development and amivantamab, a bispecific molecule targeting epidermal growth factor receptor (EGFR) and cMET that is partnered with Janssen, was recently approved by the FDA to treat adult patients with locally advanced or metastatic non-small cell lung cancer.[22]

As diseases are complex in nature and originate from a multitude of factors and mediators, the biopharmaceutical industry is interested in developing molecules with more than two specificities,[23–26] but this involves additional complexities in protein engineering.[27] In this regard, our group recently developed a platform process to generate multispecific antibodies with flexible valencies by exchanging VH and VL of a conventional Fab with camelid derived VHH single domain antibodies.[28] By applying SEED for heavy chain heterodimerization, trispecific antibodies have readily been produced.

In this study, we investigated whether cFAE can be applied to generate antibodies with up to four specificities. For this, one c-MET and one HER2 targeting antibody were equipped with F405L and K409R mutations, respectively. Different VHHs directed against EGFR, interleukin 6 receptor (IL6R) and natural killer group 2D receptor (NKG2D) were fused to the C-termini of each antibody (via a 15 aa GS-linker) and guided through cFAE, which results in up to tetraspecific antibodies (termed DB-VHH; Figure 1). A multitude of different DB-VHHs were produced and analyzed for their manufacturability characteristics. In addition, we were able to demonstrate simultaneous binding by using biophysical and cell-binding assays, as well as NK cell redirection resulting in robust tumor cell killing. Taken together our data indicate that cFAE can be applied for the generation of tri- and tetraspecific antibodies with flexible valencies.

Results

Experimental Design

In this study we aimed to explore whether cFAE can be applied for the generation of complex multispecific antibody constructs. These consist of an "IgG-like bispecific" module, whose C-termini are fused to different VHH molecules via a GS-linker (sequence: (Gly-Gly-Gly-Gly-Ser)$_3$) (Figure 1). This linker provides flexibility and mobility of the connected domains due to the utilization of small amino acids. In addition, stability of the linker in aqueous solutions is mediated by the incorporated serine residues that form hydrogen bonds with water molecules and reduce interactions between the connected domains and the peptide linker.[29] Two mAbs targeting cancer-related receptors were used as model antibodies: Trastuzumab K409 (anti-HER2) and CS06 F405L (anti-c-MET),[30,31] together with previously described VHHs against EGFR (9G8 nanobody),[32] IL6R[33] and NKG2D.[34] In sum, 8 different parental molecules (Figure S1) were produced with Fc-silencing mutations (L234A/L235A).[35] Afterward, these constructs were recombined by cFAE. Parental and recombined DB-VHHs generated in this manner, are schematically represented in Figure S1 and Figure S2.

Expression, Purification and Analytics of the Parental IgG-VHHs

Parental molecules were expressed in Expi-CHO-S cell cultures and purified by standard MabSelect affinity chromatography. Reasonable yields (35–150 mg/l) were obtained for all molecules (Table 1), and analytical size exclusion chromatography (SEC) confirmed a high purity and a low aggregation profile. In addition, melting temperatures were approximately 65°C for CS06-based and 71°C for trastuzumab-based antibodies, indicating no decrease in thermal stability of VHH-fused constructs compared to IgGs.

Recombination and Analytics of DB-VHHs

For cFAE, parental molecules were mixed at a 1:1 molar ratio and reduced with 75 mM 2-MEA and incubated for 5 h at 31°C. Afterward, the reducing agent was removed using a desalting
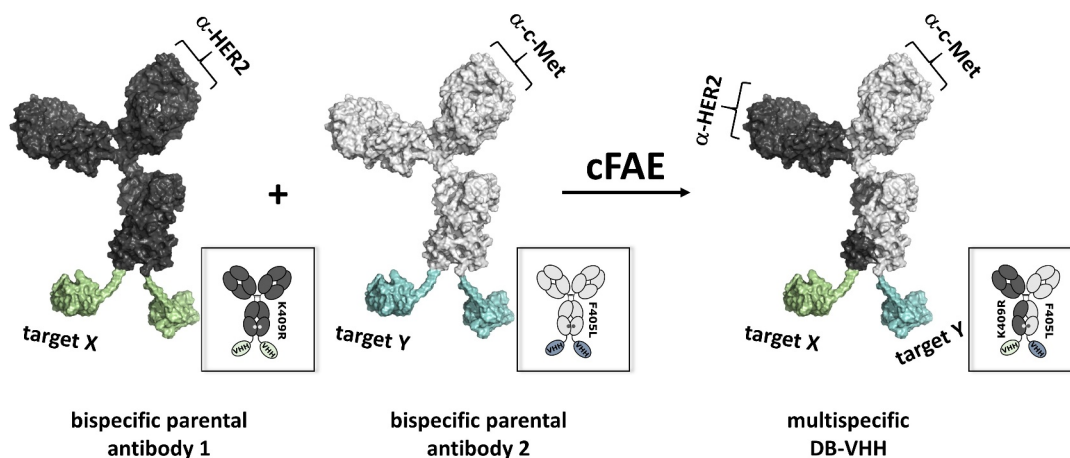
Figure 1. Generation of multispecific DB-VHH constructs. Trastuzumab IgG1-K409R mAb (anti-HER2) C-termini are fused to VHHs directed against EGFR, IL6R or NKG2D via a GS-linker. CS06 IgG1-F405L mAb (anti-c-MET) is fused to the same VHH molecules in the same manner. After recombinant production and purification, parental IgG-VHHs are recombined pairwise by reduction and reoxidation. The matching K409R and F405L mutations drive the generation of heterodimeric multispecific DB-VHHs.

Table 1. Recombinant expression and purification of parental DB-VHH molecules.

Nr.	Sample	Yield (mg/l)	Endotox (EU/mg)	Tm (°C)	SE-HPLC MabSelect purity (%)	SE-HPLC Final purity (%)	Calc. MW (kDa)
1	CS06 F405L	74.1	0.46	64.9	93.8	96.1	144.5
2	CS06 F405L-a-EGFR VHH	34.8	0.52	65.3	93.3	96.3	174.4
3	CS06 F405L-a-IL6R VHH	86.9	0.53	66.1	93.7	96.5	172.4
4	CS06 F405L-a-NKG2D VHH	108.0	0.09	64.9	93.0	96.1	173.8
5	Trastuzumab K409R	96.6	0.09	70.5	94.7	100	145.1
6	Trastuzumab K409R-a-EGFR VHH	136.8	0.04	72.1	96.	100	175.0
7	Trastuzumab K409R-a-IL6R VHH	143.9	0.29	71.7	96.3	99.3	173.0
8	Trastuzumab K409R-a-NKG2D VHH	150.9	0.07	70.4	95.8	100	174.5

column, and samples were stored overnight at 4°C for reoxidation of disulfide bonds. Efficiency of cFAE was measured using hydrophobic interaction chromatography (HIC) (Figure 2a-c). Due to the distinct hydrophobicity profiles of the trastuzumab- and CS06-based parentals, the formation of the DB-VHHs, consisting of 50% of each parental antibody, could easily be monitored. The retention times of the reassembled multispecific DB-VHHs are between those of the two parental molecules. HIC analysis revealed a high recombination efficiency for anti-NKG2D- and anti-EGFR-based antibodies (>90%), whereas heterodimerization of anti-IL6R-VHH harboring molecules was not as efficient (80%–85%; Table 2). Lower absorption units of CS06 were observed due to instabilities of this antibody in the 1 M ammonium sulfate HIC buffer.

The physicochemical properties of the recombined molecules were further examined via SEC and melting point analysis (Tm). The SEC (Figure 2d-f) showed no undesired aggregation or fragmentation after the recombination process, and melting temperatures were comparable to those of the parental molecules (Table 2). This indicates no detectable decrease in stability of the antibodies following reduction and reoxidation.

Functional Characterization of DB-VHHs

Affinity and Simultaneous Antigen Binding
Binding kinetics of parentals and recombined DB-VHHs to their corresponding antigens were measured using biolayer interferometry (BLI). Affinities (equilibrium dissociation constants (KDs)) of the bivalent trastuzumab and CS06 parental molecules to recombinant HER2 and c-MET, respectively, lay in the sub-nanomolar range (Table 3), which is comparable to previous reports.[31,36] Following cFAE, no significant change in c-MET and HER-2 binding was observed for all DB-VHHs (Table 3).

The three VHH molecules differed in their binding affinities toward their antigens. The VHH directed against IL6R exhibited the highest affinity with subnanomolar KDs, followed by the NKG2D-targeting VHH (~5 nM). The weakest interaction to its antigen was measured for the anti-EGFR VHH, with KDs in the double-digit nanomolar range. As for the c-MET and HER2 paratopes, no significant differences in affinity of the mono- and bivalent format was observed for the VHH modules. In sum, all DB-VHHs bound their antigens comparable to the parental antibodies (Figure S3-S7) and independently of their valency (Table 3). In addition, we also tested affinities of VHHs fused to the N-terminus of either a SEED (one armed; anti-EGFR and anti-NKG2D) or a Fc (bivalent; anti-IL6R) (Table S1; Figure S7). While the C-terminal fusion of the IL6R-VHH in the DB-VHH format did not result in diminished affinity, anti-EGFR and anti-NKG2D paratopes showed a reduced affinity by a factor of 10 when comparing N- to C-terminal Fc fusion. Such positioning effects of antibodies and antibody fragments are well known and have also been reported for molecules such as DVD-Igs and on a functional level for CODV molecules.[37,38]

In several therapeutic settings, multispecific antibodies need to bind their targets simultaneously. To demonstrate the ability of the recombined constructs to address multiple antigens concomitantly, BLI measurements were performed, wherein association of the respective protein to multispecific antibodies was measured in a sequential manner (Figure 3 and Figures S8-S10). Strong interference shifts were detected during association of the DB-VHH constructs to c-MET, which was immobilized to the biosensors. At the same time, no unspecific interaction between the biotinylated c-MET-immobilized biosensors with trastuzumab wildtype could be detected (Figure 3a,c). Successive association of IL6R, NKG2D, EGFR and HER2 proteins to DB-VHHs was confirmed using a control biosensor in kinetic buffer (KB) as a reference. Since dissociation of the antibody constructs from c-MET, and thus from the biosensor, counteracts the association of the remaining antigens, reduced binding signals were obtained throughout the assay. Nevertheless, a specific interaction between all VHHs and tested antigens, as well as HER2 binding via the trastuzumab-Fab could be detected, demonstrating simultaneous binding of all DB-VHHs.

Target Cell Binding
Specific target cell binding was assessed using parental antibodies and tumor cell lines expressing the respective receptor (Figure 4). All antibodies comprising a trastuzumab moiety demonstrated strong binding to HER2-overexpressing HCC-1954 cells, whereas no binding of the CS06-Fabs or the VHH-binding sites of the remaining constructs could be detected. Similarly, the EBC-1 cell line, which is characterized by MET gene amplification, was specifically bound by the CS06 constructs only.[39] Here, a slight binding of the trastuzumab-EGFR VHH construct could be detected, which is consistent with the moderate EGFR expression of this cell line.[31] Specific binding of the anti-EGFR and anti-IL6R VHHs to EGFR-overexpressing MDA-MB-468 cells and IL6R-displaying THP-1 monocytes were verified using the same experimental procedure (Figure 4).

Simultaneous Cell Binding and Clustering
In order to demonstrate the ability of multispecific DB-VHHs to specifically engage and cluster different cell types, fluorescently stained HCC-1954, EBC-1 and MDA-
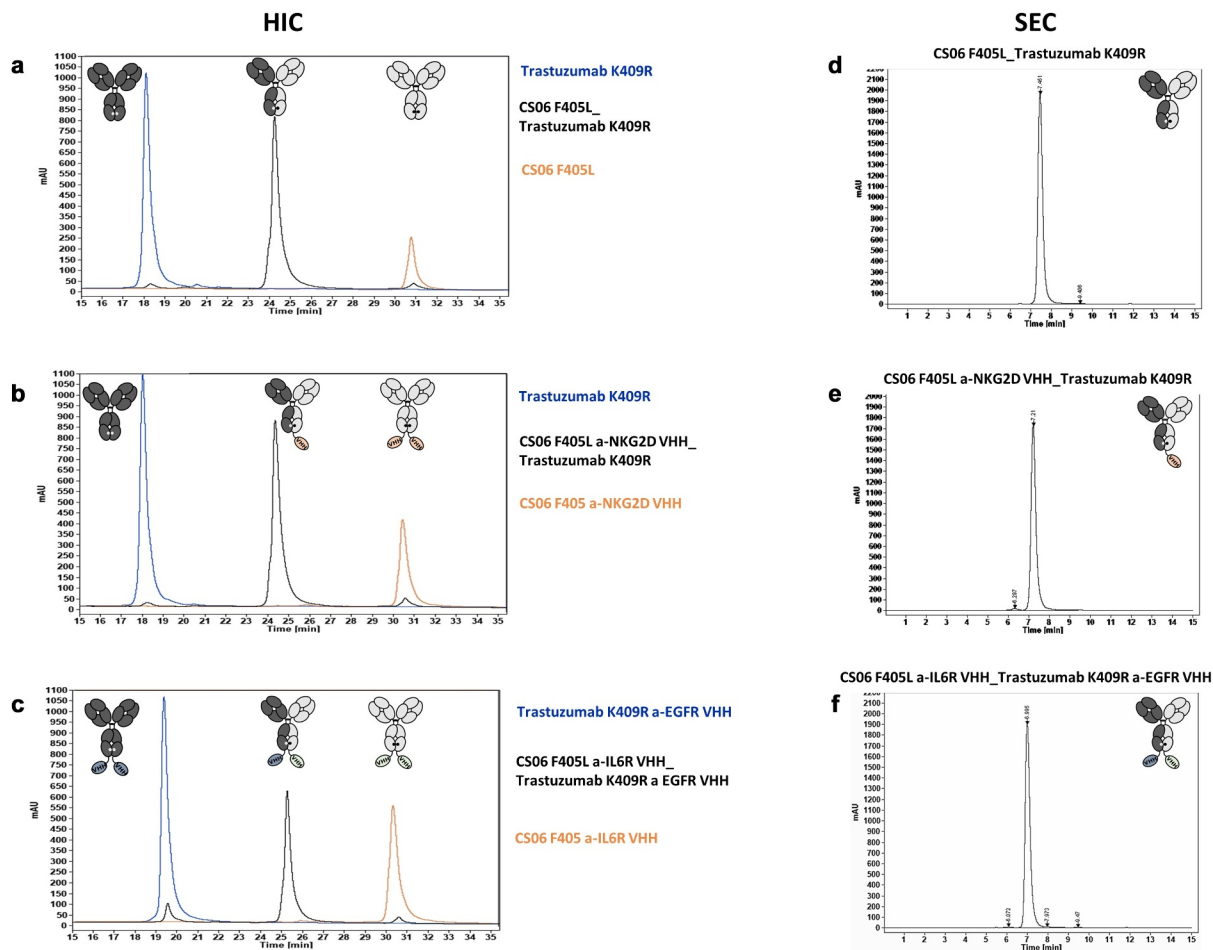
Figure 2. (a-c) Hydrophobic Interaction Chromatography (HIC) for analysis of DB-VHHs recombination efficiency. Recombined molecules exhibit hydrophobicity profiles exactly between the two parental molecules. (d-f) Size Exclusion Chromatography (SEC) for analysis of possible aggregation and fragmentation following the recombination procedure.

Table 2. Controlled Fab arm exchange and analytics of DB-VHHs.

Nr.	Sample	Endotox (EU/mg)	HIC purity (%)	Tm (°C)	SE_HPLC purity (%)	Calc. MW (kDa)
9	CS06 F405L_Trastuzumab K409R	0.28	91.2	67.1	99.0	144.8
10	CS06 F405L a-NKG2D VHH_ Trastuzumab K409R a-NKG2D VHH	0.16	90.8	72.5	97.4	174.2
11	CS06 F405L a-NKG2D VHH_Trastuzumab K409R	0.16	91.23	66.7	96.8	159.5
12	CS06 F405L a-IL6R VHH_Trastuzumab K409R	0.36	83.31	67.5	98.0	158.8
13	CS06 F405L a-EGFR VHH_Trastuzumab K409R	0.26	92.21	67.0	97.9	159.8
14	CS06 F405L_Trastuzumab K409R a-NKG2D VHH	0.27	93.59	66.3	97.9	159.5
15	CS06 F405L_Trastuzumab K409R a-IL6R VHH	0.63	82.36	67.5	89.0	158.8
16	CS06 F405L_Trastuzumab K409R a-EGFR VHH	0.70	92.91	66.8	98.0	159.8
17	CS06 F405L a-NKG2D VHH_Trastuzumab K409R a-IL6R VHH	0.22	82.83	68.2	96.6	173.4
18	CS06 F405L a-NKG2D VHH_Trastuzumab K409R a-EGFR VHH	0.10	93.94	65.6	97.4	174.4
19	CS06 F405L a-IL6R VHH_Trastuzumab K409R a-EGFR VHH	0.19	84.16	68.2	96.7	173.7

MB-468 cells were mixed and incubated in the presence of DB-VHHs with and without an EGFR-targeting VHH moiety (Figure 5). As expected, the bispecific construct (CS06 F405L_Trastuzumab K409R) bound to c-MET and HER2 receptors on EBC-1 and HCC-1954 cells, respectively, and mediated strong cell clustering (double-fluorescent events in the upper right gate, Figure 5b). Simultaneously, a large proportion of triple-fluorescent events (marked in red) was present only in case of the DB-VHHs bearing an anti-EGFR VHH. This indicates simultaneous engagement of all three cell lines through binding of the constructs to the target receptors on the cell surfaces (Figure 5c-f).

The same experiment was performed using IL6R-displaying THP-1 cells and DB-VHHs targeting IL6R via the C-terminal VHH unit. Even though the constructs mediated the formation

Table 3. Binding affinities measured for each paratope using recombinant antigens.

Nr.	Construct	Paratope 1	KD (nM) paratope 1	Paratope 2	KD (nM) paratope 2	Paratope 3	KD (nM) paratope 3	Paratope 4	KD (nM) paratope 4
1	CS06 F405L	c-MET	0.372 ± 0.006	–	–	–	–	–	–
2	CS06 F405L-a-EGFR VHH	c-MET	0.547 ± 0.008	EGFR	17.740 ± 0.144	–	–	–	–
3	CS06 F405L-a-IL6R VHH	c-MET	0.255 ± 0.009	IL6R	0.461 ± 0.008	–	–	–	–
4	CS06 F405L-a-NKG2D VHH	c-MET	0.372 ± 0.007	NKG2D	5.171 ± 0.092	–	–	–	–
5	Trastuzumab K409R	HER2	0.289 ± 0.009	–	–	–	–	–	–
6	Trastuzumab K409R-a-EGFR VHH	HER2	0.203 ± 0.012	EGFR	22.140 ± 0.160	–	–	–	–
7	Trastuzumab K409R-a-IL6R VHH	HER2	0.242 ± 0.020	IL6R	0.705 ± 0.021	–	–	–	–
8	Trastuzumab K409R-a-NKG2D VHH	HER2	0.332 ± 0.013	NKG2D	5.712 ± 0.126	–	–	–	–
9	CS06 F405L_Trastuzu K409R	c-MET	0.271 ± 0.004	HER2	0.566 ± 0.016	–	–	–	–
10	CS06 F405L a-NKG2D VHH_ Trastuzumab K409R a-NKG2D VHH	c-MET	0.247 ± 0.004	HER2	0.466 ± 0.013	NKG2D	4.229 ± 0.054	–	–
11	CS06 F405L a-NKG2D VHH_ Trastuzumab K409R	c-MET	0.229 ± 0.006	HER2	0.487 ± 0.016	NKG2D	5.433 ± 0.068	–	–
12	CS06 F405L a-IL6R VHH_ Trastuzumab K409R	c-MET	0.255 ± 0.014	HER2	0.334 ± 0.015	IL6R	0.685 ± 0.011	–	–
13	CS06 F405L a-EGFR VHH_ Trastuzumab K409R	c-MET	0.285 ± 0.005	HER2	0.381 ± 0.014	EGFR	22.950 ± 0.221	–	–
14	CS06 F405L_ Trastuzumab K409R a-NKG2D VHH	c-MET	0.217 ± 0.012	HER2	0.111 ± 0.016	NKG2D	5.303 ± 0.120	–	–
15	CS06 F405L_ Trastuzumab K409R a-IL6R VHH	c-MET	0.205 ± 0.004	HER2	0.467 ± 0.020	IL6R	0.807 ± 0.010	–	–
16	CS06 F405L_ Trastuzumab K409R a-EGFR VHH	c-MET	0.270 ± 0.005	HER2	0.403 ± 0.014	EGFR	22.270 ± 0.146	–	–
17	CS06 F405L a-NKG2D VHH_ Trastuzumab K409R a-IL6R VHH	c-MET	0.337 ± 0.005	HER2	0.436 ± 0.015	NKG2D	4.502 ± 0.054	IL6R	0.973 ± 0.013
18	CS06 F405L a-NKG2D VHH_ Trastuzumab K409R a-EGFR VHH	c-MET	0.221 ± 0.006	HER2	0.378 ± 0.017	NKG2D	5.081 ± 0.068	EGFR	22.140 ± 0.160
19	CS06 F405L a-IL6R VHH_ Trastuzumab K409R a-EGFR VHH	c-MET	0.113 ± 0.008	HER2	0.262 ± 0.015	IL6R	0.414 ± 0.014	EGFR	52.900 ± 1.965
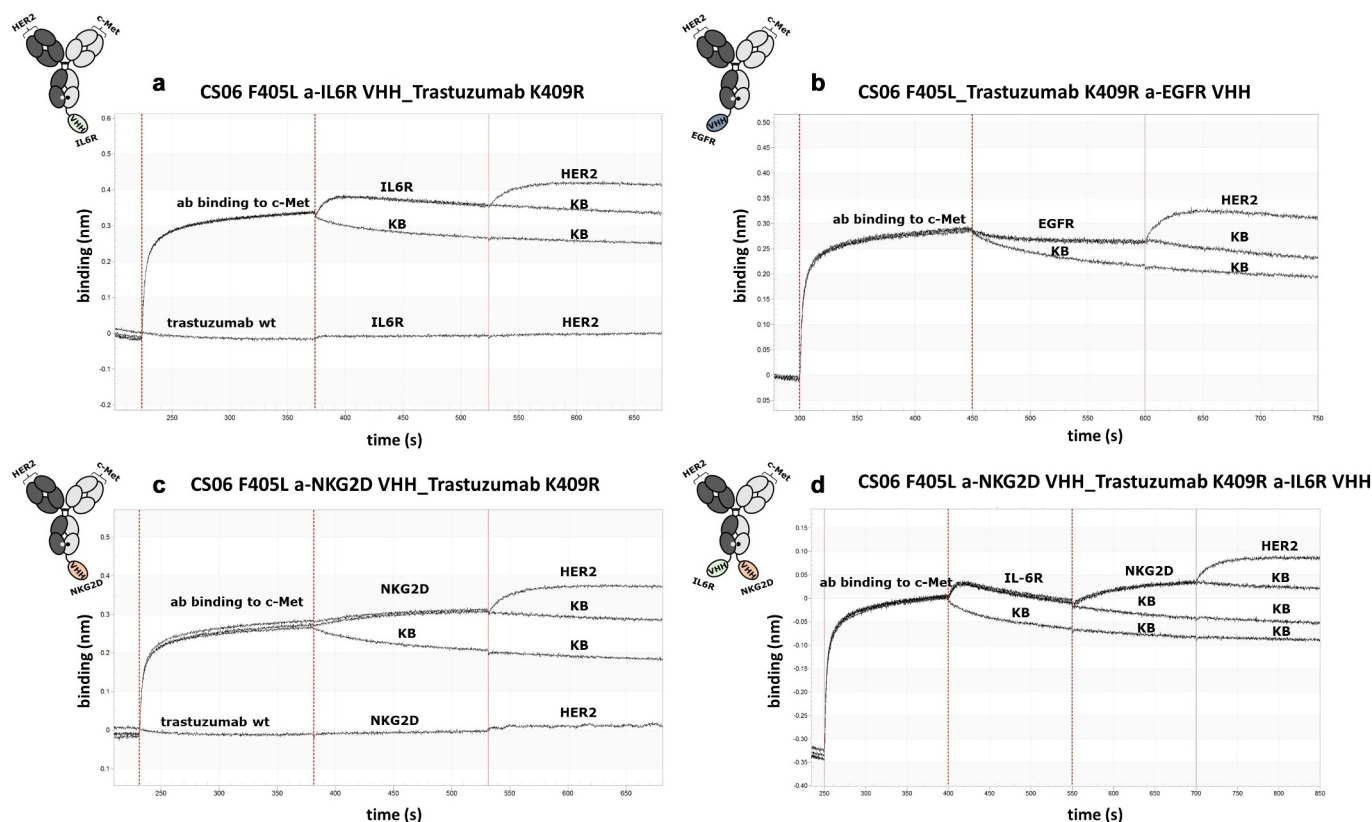
Figure 3. Biolayer interferometry analysis of simultaneous antigen binding of tri- and tetraspecific DB-VHHs. (a), (b) and (c) show exemplary sensorgrams for trispecific molecules and (d) a tetraspecific DB-VHH. The first association step represents binding of the DB-VHH (200 nM) via its CS06 paratope to biotinylated c-MET immobilized to streptavidin biosensors. Second (and third for (D)) association step is performed using an IL6R, EGFR or NKG2D recombinant protein (200 nM). The last association step is performed using HER2 (200 nM). Kinetic buffer (KB) controls were applied as negative controls for each association step.
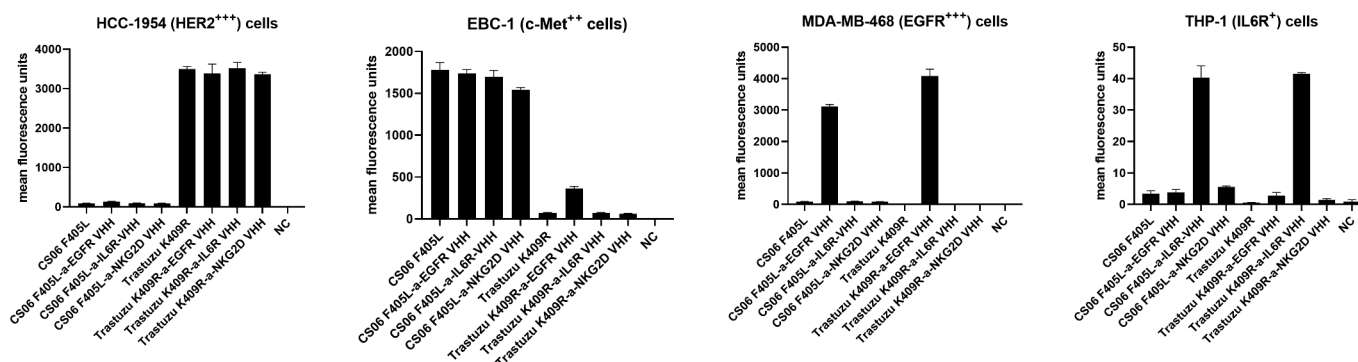
Figure 4. Binding of the parental IgG-VHH constructs to tumor cell lines. Cells were incubated with 100 nM IgG-VHH construct and binding was detected using a fluorescently labeled detection antibody. Cells were analyzed via flow cytometry, and the normalized mean fluorescence signal of three biological replicates was plotted for each construct.

of HCC-1954 + EBC-1 cell doublets, no significant engagement of the THP-1 cell line could be detected (Figure S11; Figure S12). To examine if the binding of the anti-IL6R VHH to its antigen is impaired due to the interactions of the constructs with membrane-associated HER2 and c-MET receptors, we incubated mixed HCC-1954 and EBC-1 cells with the constructs in the presence of recombinant IL6R (Figure 6). In this case, more than 80% of the clustered HCC-1954 + EBC-1 cells were simultaneously labeled with recombinant IL6R (events marked in blue). This indicates non-impaired binding of the respective VHH to recombinant IL6R (Figure 6).

### Physiological Activity: NK Cell Activation

To investigate the functional activity of the multispecific antibody format, a cytotoxic NK cell-mediated lysis assay was performed using the constructs comprising a NKG2D-targeting domain. Prior to the killing experiment, NKG2D-mediated target cell clustering as well as cell binding was analyzed and confirmed (Figure S13; Figure S14). Specific target cell lysis by peripheral blood mononuclear cell (PBMC)-isolated NK cells was observed for both parental and recombined anti-NKG2D DB-VHHs (Figure 7 black plots). As expected, no killing of SK-BR-3 cells was observed when incubated with the c-MET targeting IgG-VHH (Figure 7c red plot). This indicates that specific target cell engagement is necessary for NK cell-mediated killing. Interestingly, the trastuzumab-containing constructs devoid of an NKG2D-binding VHH still showed NK cell-mediated SK-BR-3 cell lysis at high concentrations, regardless of the incorporated Fc-silencing mutations (LALA) (Figure 7c,d violet plots). This phenomenon was not observed on EBC-1 cells or with molecules carrying the anti c-MET paratope and SK-BR-3 cells (Figure 7a-violet plot and Figure 7c and 7d-red plots). In sum, these findings demonstrate that cFAE can be applied to generate functional multispecific antibodies that can engage NK cells for tumor cell lysis.

Discussion

Most strategies for the generation of bsAbs rely on either genetic fusion or co-expression of different chains.[40,41] Fc-bearing molecules require several mutations for heavy chain heterodimerization and correct light chain assembly and complex downstream processes to reach high product purity.

Compared to conventional methods, cFAE makes use of only one mutation per CH3 domain, which strongly favors heterodimerization after reduction of the two parental antibodies.[19,21,42] The main advantage of cFAE is the maintained VH-VL pairing.[20] Therefore, VH-VL pairs that are derived from any discovery campaign can directly be used for cFAE without additional protein-engineering efforts. As recently reported, camelid-derived single-domain antibodies can also be used as one binding domain in DB.[43] By exchanging one Fab by a VHH module, Huang et al.[43] were able to show high product purity of the VHH/Fab bispecific DuoBody format for three different model antibodies. Here, we investigated whether VHHs can be applied to generate multispecific antibodies in the DuoBody context. For this, three different antibody fragments were C-terminally fused to two different mAbs by a 15 aa GS-linker. Production yields and SEC purity of the generated IgG-VHH fusions were comparable to that of the CS06 and trastuzumab IgGs. Initially, it was tempting to speculate that direct fusion of a protein to DuoBody CH3 domains may lead to steric hindrance during cFAE. We did not detect any interference of C-terminally fused anti-EGFR and NKG2D antibody fragments on chain reassembly, as heterodimerization efficiency was calculated to be above 90% (Table 2) using the standard cFAE procedure. However, for the anti-IL6R fusion proteins, quantities of heterodimers were only in the range of 80%. Interestingly, the *in silico* predicted hydrophobicity surface patch area and aggregation-prone regions score (derived from a three-dimensional (3D) model of the IL6R-binding VHH) of this antibody was significantly higher than those of the two other VHHs (Figure S15A). Hydrophobic intramolecular interactions between both IL6R-binding VHHs in the DB-VHH homodimer might prevent full dissociation and thereby hinder complete heterodimerization. This hypothesis is in agreement with a molecular dynamics (MD) simulation that was performed for the parental DB-VHH CS06 F405L-a-IL6R VHH and suggests an association of both VHH domains, which is maintained until the end of the simulation (Figure S15B).

Our group recently reported a VHH-based technology for the generation of IgG-like multispecific antibodies. In this study, VH and VL of a Fab fragment were exchanged by VHHs with different specificities.[28] The versatility of this format was demonstrated with the functional production of
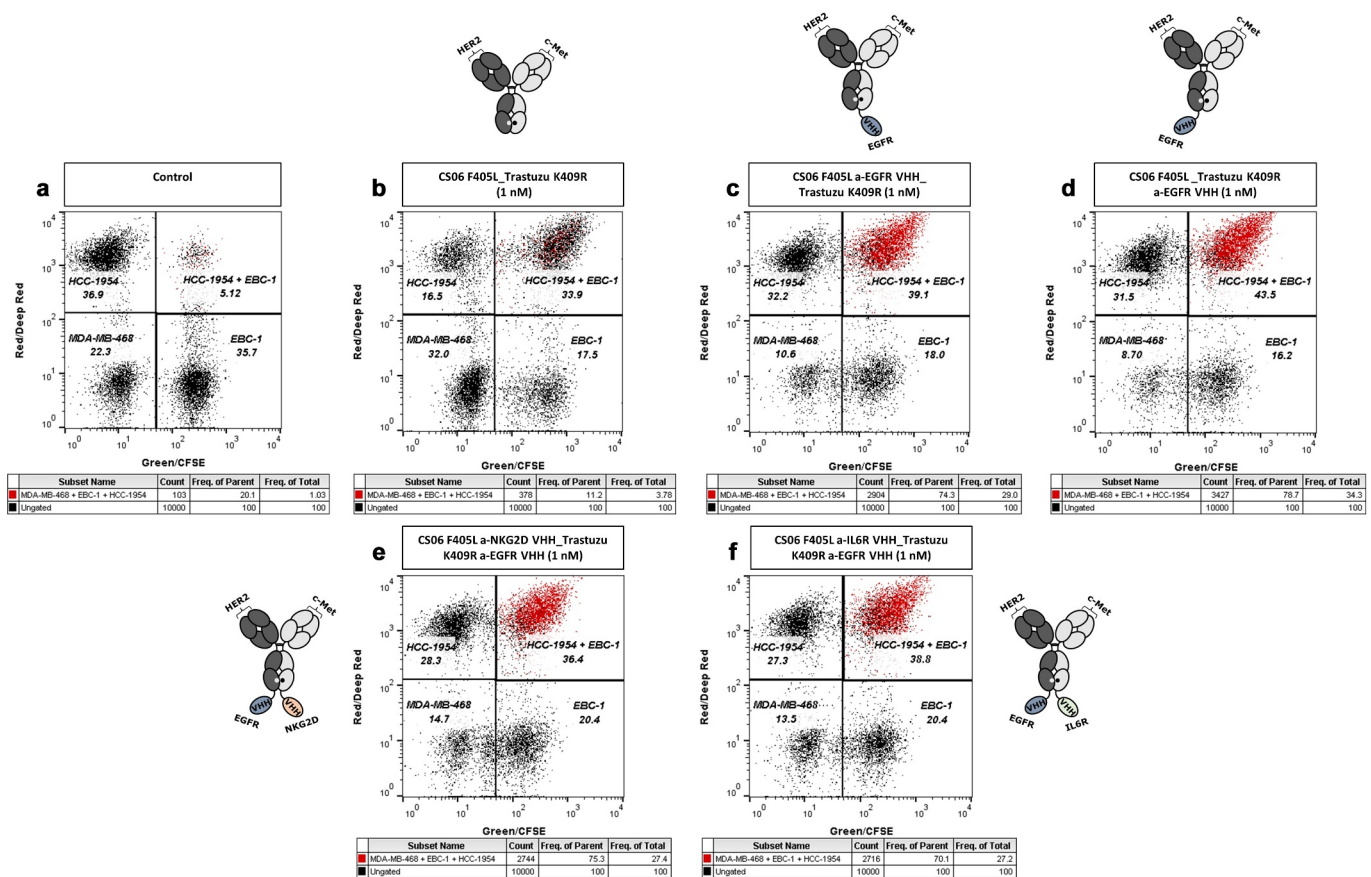
Figure 5. Specific cell clustering due to simultaneous binding of the DB-VHHs to three different cancer cell lines. Flow cytometry cytograms represent the fluorescence signals of the different cell populations. (a) Cells without antibody construct. Upper left gate = HCC-1954 (HER2^{+++}) cells stained with DeepRed, lower left gate = MDA-MB-468 (EGFR^{+++}) cells stained with CMRA, lower right gate = EBC-1 (c-MET^{++}) cells stained with CFSE, upper right gate = HCC-1954 + EBC-1 cell doublets. Events in all three fluorescence channels (cell triplets) were marked in red. Cells were incubated in the presence of 1 nM (b) bispecific DB, (c) and (d) trispecific DB-VHHs, (e) and (f) tetraspecific DB-VHHs.

a variety of constructs but is limited to trispecific antibodies, in which the light chain encoded VHH is bivalent. In contrast, the herein described DB-VHH format can lead to tri- (mono or bivalent) and tetraspecific antibodies (Figure S2). We were able to show simultaneous binding of all generated constructs to their respective recombinant antigens via BLI (Figure S4-S7). Moreover, simultaneous engagement of up to three antigen-positive cell lines was assessed with DB-VHHs carrying c-MET/HER2 and EGFR specificities (Figure 5). In terms of the c-MET/HER2/IL6R-targeting DB-VHH, only HCC-1954 and EBC-1 efficiently clustered without co-engagement of THP-1 cells (Figure S12). It is possible that, due to steric hindrance, the IL6R paratope is not able to interact with cellularly expressed IL6R. Nevertheless, DB-VHHs were still able to co-engage recombinant IL6R in the cellular setting, demonstrating integrity of each paratope (Figure 6).

Finally, we aimed to explore the functionality of multispecific DB-VHHs. For this, the anti-NKG2D-VHH-carrying DBs were used in a NK cell-mediated tumor cell cytotoxicity assay. c-MET-expressing EBC-1 cells and HER2-expressing SK-BR-3 cells were specifically killed by NK cells when incubated with NKG2D-fusion proteins (Figure 7). In terms of SK-BR-3 cells, NK cell-mediated lysis was also observed with the effector-silenced trastuzumab-LALA variant in the parental, as well as in the trispecific format without the NKG2D moiety (Figure 7c,d). Similar antibody-

dependent cell-mediated cytotoxicity (ADCC) effects of trastuzumab-LALA have been previously reported.[44] While PG-LALA completely abolishes FcγRIIIa binding, LALA retains some CD16a activation.[35] The fact that this effect was only seen with trastuzumab-based antibodies on SK-BR-3 cells and not with CS06-LALA antibodies and EBC-1 cells might be explained by the much lower c-MET surface receptor density. While SK-BR-3 cells carry roughly 1.5 million HER2 receptors per cell, EBC-1 cells display about 0.25 million copies of c-MET.[45,46] The positive effect of surface receptor density on ADCC was described in detail by Cleary et al.[47] in 2017.

Taken together, our data indicate that single domain antibodies in combination with cFAE can be applied for the generation of functional multispecific antibodies.

Multispecific antibodies are becoming attractive modalities as, for example, novel immune-oncological therapies. As an example, Sanofi recently reported preclinical data for a trispecific CODV targeting CD38 on cancer cells and CD3 as well as CD28 on T cells.[25] They experimentally demonstrated that the dual activation signal (CD3 and CD28) is required to stimulate T-cells for optimal effector function and proliferation. Known as SAR442257, this antibody is now being evaluated in a Phase 1 clinical study (NCT04401020). Multispecific targeting of activating immune cell receptors, however, comes with the risk of so-called fratricide. It is proposed that crosslinking of receptors on immune cells may lead
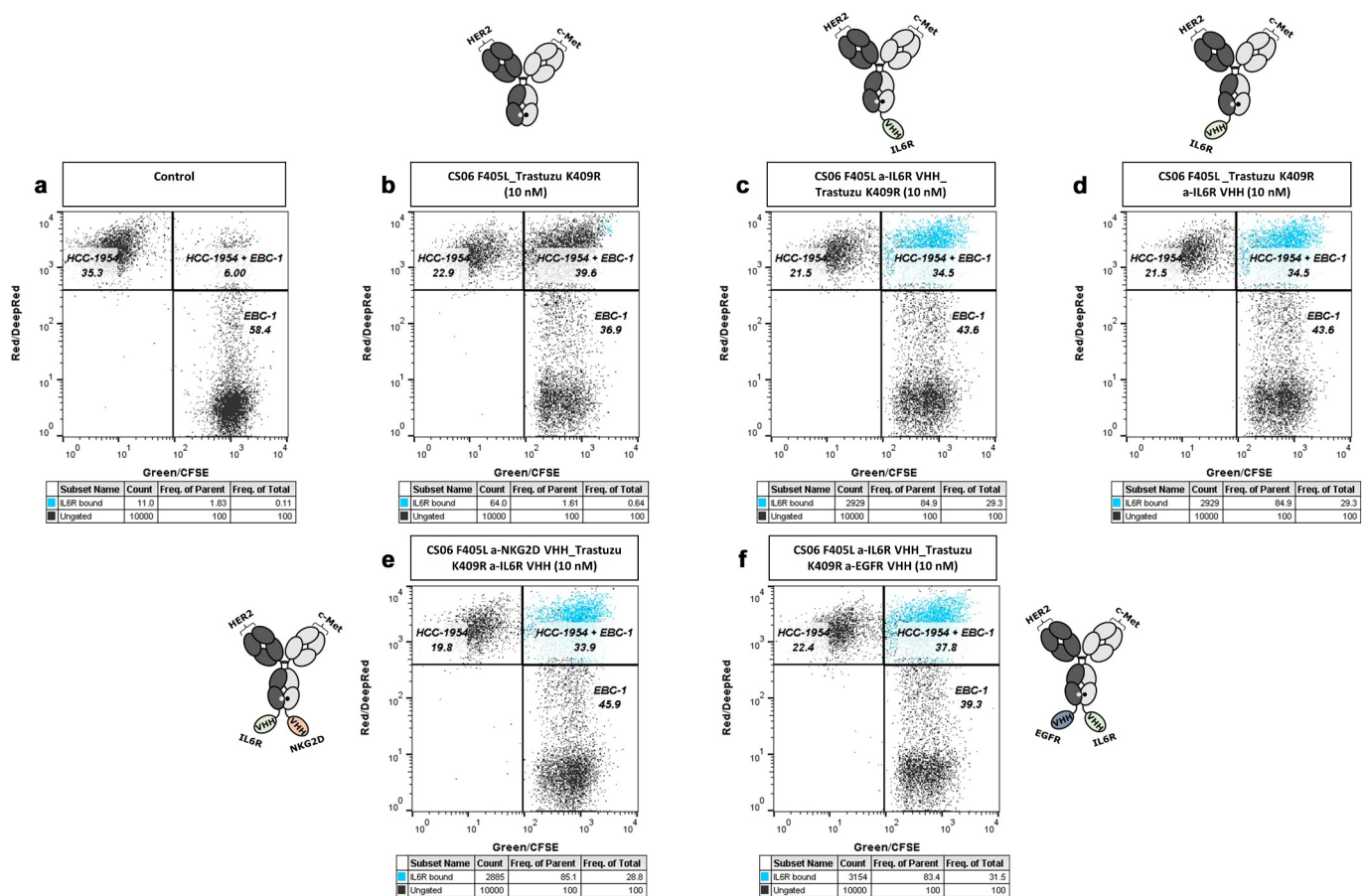
Figure 6. Simultaneous interaction of the DB-VHHs with HCC-1954 and EBC-1 target cells and binding of recombinant IL6R. Flow cytometry cytograms represent the fluorescence signals of the two cell populations and bound recombinant IL6R, detected with an anti-His6 detection antibody. (a) Cells without antibody construct. Upper left gate = HCC-1954 (HER2+++) cells stained with DeepRed, lower right gate = EBC-1 (c-MET++) cells stained with CFSE, upper right gate = HCC-1954 + EBC-1 cell doublets. Events in all three fluorescence channels (HCC-1954 + EBC-1 + bound recombinant IL6R-His Tag) were marked in blue. Cells were incubated in the presence of 10 nM (b) bispecific DB, (c) and (d) trispecific DB-VHHs, (e) and (f) tetraspecific DB-VHHs.

to depletion of specific immune-cell subsets.[48] Whether fratricide will be a safety concern of multispecific antibodies in the clinical setting will be demonstrated by the outcome of Phase 1 studies.

The antibody format seems to be acceptable in terms of (early) developability and all tested paratopes were able to simultaneously engage in antigen binding. One limitation of the herein described technology might be the application of hydrophobic VHHs as C-terminal antibody fusion. In case of the IL6R targeting VHH, insufficient heterodimerization was observed, likely due to intramolecular hydrophobic interactions of both VHHs in the parental DuoBody. Nevertheless, taking this into consideration, we believe that cFAE can be applied to generate multispecifics without complex protein engineering. In contrast, other bi- and multispecific formats like DARTs, DVD-Igs as well as CODV-Igs often require complex optimization to yield molecules with good manufacturability and binding characteristics.[37,38,49]

In conclusion, DB-VHHs expand the toolbox of conventional DB in a plug and play manner and might be of interest for the development of complex therapeutics in the future.

Materials and Methods

Recombinant Expression and Purification of Parental Antibodies

Genetic constructs were purchased in a standard pTT5 vector (GeneArt/Thermo Fisher Scientific) for antibody expression in mammalian cell culture. All antibodies were expressed using the ExpiCHO Expression System Kit (Thermo Fisher, Cat. A29133) according to the manufacturer's protocol. Transfections were harvested on day 6 post-transfection, and cells and supernatant were separated by centrifugation (Multifuge 3-R, Heraeus) at 4300 x g for 20 minutes at 4°C. Supernatants were filtered through a 0.2 μm PES filter (Nalgene, 597–4520).

Antibodies were purified by Protein A affinity chromatography (HiTrap MabSelect SuRe, Cytivia) followed by a polishing step with HiLoad Superdex 200pg gel filtration (Cytivia) equilibrated in phosphate-buffered saline (PBS) pH 7.4. Antibodies were concentrated using Amicon Ultra-15 centrifugal filter devices (50 kDa, EMD Millipore) and sterile filtered (0.2 μm). Protein concentration of purified antibodies was measured using a NanoDrop One UV-Vis Spectrophotometer (Thermo Fisher) and calculated with the
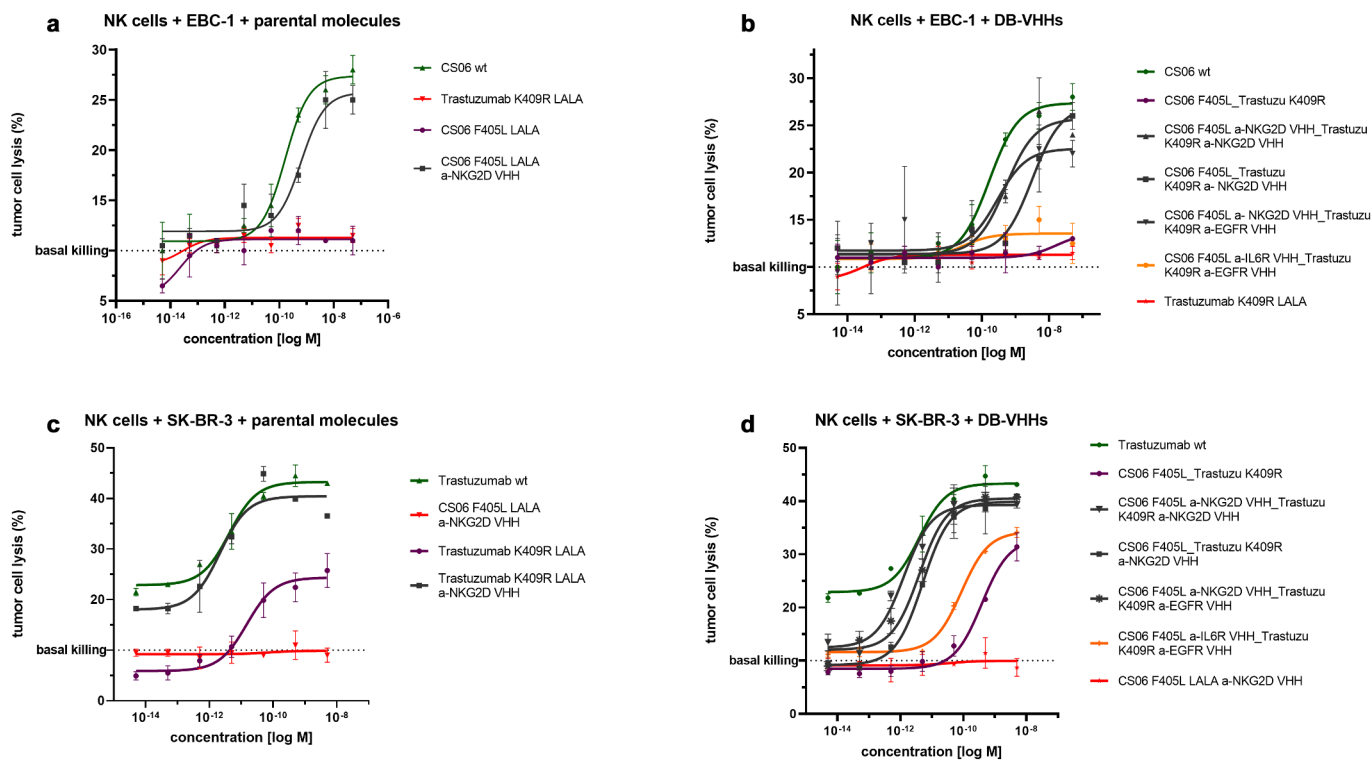
Figure 7. DB-VHHs elicit potent and specific NK cell-mediated target cell killing. Tumor cells were incubated with primary effector cells (NK cells) at a 1:5 ratio in the presence of antibody constructs in different concentrations. Error bars represent standard deviation of two biological replicates. Wildtype CS06 and trastuzumab with active Fc effector functioning were used as an ADCC reference (green). (a) and (b): c-MET-positive EBC-1 target cells, (c) and (d) HER2-overexpressing SK-BR-3 target cells. (a) and (c): NK cell cytotoxicity triggered by parental antibodies. (b) and (d): DB-VHHs serve as NK cell engager and mediate tumor cell killing.

extinction coefficient based on the amino acid sequence. The quality of the purified antibodies was assessed using SDS-PAGE reduced and non-reduced (Invitrogen) (data not shown), high-performance size-exclusion chromatography (SE-HPLC) using TSKgel SuperSW3000 (Tosoh Bioscience) in an Agilent HPLC system, and an Endosafe Nexgen-PTS system (Charles River) for determining the endotoxin levels.

Recombination and Re-Oxidation of DB-VHHs

Parental molecules were mixed at a 1:1 molar ratio, adjusted to a final protein concentration of 2 mg/ml in PBS pH 7.4 and reduced with 75 mM 2-MEA (cysteamine hydrochloride BioXtra, Sigma Aldrich) from a freshly prepared 750 mM 2-MEA stock solution. Samples were mixed for 5 min on a rotating mixer at ambient temperature and further incubated for 5 h at 31°C. To remove the reducing agent, samples were desalted in PBS pH 7.4 using HiPrep 26/10 desalting column (Cytivia). Samples were stored overnight at 4°C to allow for the re-oxidation of the disulfide bonds.

Hydrophobic Interaction Chromatography Analysis of DB-VHHs

HIC was performed on Butyl-NPR (2.5 μm 4.6 mm x 100 mm) column (TOSOH Bioscience 42168) at 25°C. Protein samples formulated in PBS pH 7.4 were mixed with ammonium sulfate at 1 M end concentration and analyzed at a flow rate of 0.75 ml/min using a linear gradient of 50 mM sodium phosphate +

1.5 M ammonium sulfate pH 7.0 to 50 mM sodium phosphate + 5% isopropanol pH 7.0 in 33 min. Typically, 20 μg of protein sample were loaded onto the column. Absorbance was monitored at 214 nm using a multi-wavelength detector (Agilent). ChemStation software (Agilent) was used to integrate the peak areas of the DB-VHH and non-recombined parental molecules and to calculate the relative peak areas.

Melting Point Measurement

The temperature stability of the molecules was measured with a Prometheus device (NanoTemper Technologies). The measurement was performed with a linear gradient from 20 to 95°C with a temperature rise of 1°C/min. The onset and melting points were calculated by the NanoTemper Analysis software. Tm1 was used as a measure of the thermal stability all molecules.

Kinetic Measurements

BLI was used for analysis of the binding kinetics of the parental and the recombined DB-VHH constructs to their corresponding antigens. All measurements were performed on Octet RED96 system (ForteBio, Pall Life Science) at 25°C and 1000 rpm agitation.

Parental antibodies and DB-VHHs were loaded on anti-human IgG Fc capture (AHC) biosensors (ForteBio) at a concentration of 5 μg/ml in PBS for 180 s or until a threshold of 1 nm was reached. The biosensors were then rinsed in kinetics

buffer (KB; PBS + 0.1% Tween-20 + 1% bovine serum albumin (BSA)) for 45 s (baseline) and the corresponding antigen was associated to the biosensor for 300 s. Different antigen concentrations (1:2 dilution rows in KB) were tested in order to identify the dynamic range of the binding kinetics and the most suitable concentration ranges were determined as follows: HER2/ErbB2 ECD-His Tag (Sino Biological, Cat: 10004- H08H) – 0.78 nM to 50 nM, c-MET ECD-strepII-His Tag (in-house production) – 0.39 nM to 25 nM, human EGFR-His Tag (ACRO Biosystems, Cat: EGR-H5222) – 1.5 nM to 100 nM, human IL6R ECD-His Tag (Sino Biological, Cat: 10398-H08H) – 0.78 nM to 50 nM, and human NKG2D-His Tag (Sino Biological, Cat: 10575-H07B) – 0.78 nM to 50 nM. Dissociation was carried out in kinetics buffer for 300 s (600 s in case of IL6R). A reference value (association in KB instead of antigen solution) was used for data analysis, and fitting was performed using the ForteBio data analysis software 8.0 (Savitzky-Golay filtering and 1:1 binding model).

Simultaneous Antigen Binding

BLI was used to examine the capability of the tri- and tetra-specific DB-VHHs to bind simultaneously all corresponding antigens as well. For this purpose, c-MET was biotinylated using EZ-Link Sulfo-NHS-LC-Biotinylation Kit (Thermo Fisher Scientific, Cat: 21435) according to the manufacturer's protocol. Briefly, 280 µg recombinant c-MET (in-house) was mixed with 20 molar equivalents sulfo-NHS-biotin in 100 µl PBS. The biotinylation reaction was carried out for 2 h on ice and the excess biotin was removed using two Zeba Spin Desalting Columns 7 K MWCO (Thermo Fisher Scientific, Cat: 89882). C-MET-biotin (100 nM in PBS) was loaded for 200 s on Streptavidin (SA) biosensors. Next, free streptavidin binding sites were blocked for 60 s with blocking solution consisting of 1% skimmed milk powder, 1% bovine serum albumin (BSA), 0.1% Tween-20 and 10 µg/ml biocytin in PBS. The biosensors were rinsed in KB for 120 s (baseline) and the DB-VHHs (200 nM in KB) were associated for 180 s. This first step represents binding of the CS06-Fab to the c-MET antigen. The following association steps were performed by dipping the biosensors in sequential manner in the antigens (200 nM in KB), addressed by the C-terminal VHH molecules (EGFR, IL6R and NKG2D) for 180 s and a final association of HER2 (200 nM in KB) to the trastuzumab-Fab for 180 s, as well.

Specific Cell Binding

Cell binding experiments were performed using the parental constructs and antigen (over)expressing tumor cells. HCC-1954 (HER2-positive), EBC-1 (c-MET-positive), MDA-MB-468 (EGFR-positive) and THP-1 (IL6R-positive) cells were trypsinized, washed twice with cold PBS + 1% BSA and seeded in a 96-well plate (1×10^5 cells/well). Cells were incubated with 100 nM parental antibody in triplicates for 1 h on ice, washed twice with cold PBS + 1% BSA and incubated for additional 1 h on ice with 200 nM detection antibody (Alexa Fluor 488 AffiniPure Fab Fragment Goat Anti-Human IgG (H + L) (Jackson ImmunoResearch, Cat: 109–547-003)). Following two washing steps, the cells were resuspended in 200 µl PBS + 1% BSA and 20 µg/ml

propidium iodide (PE) (Invitrogen) were mixed for dead cell staining. Cells treated only with detection antibody were used as a negative control (NC) and untreated cells were used for normalization of the fluorescence signal. Flow cytometry measurement was performed on Guava® easyCyte 12HT (Merck Millipore) using GuavaSoft 3.3 Software where 5000 events/well were recorded and analyzed. Mean fluorescence intensities from three biological replicates were plotted using GraphPad Prism 9.0.0 software.

Simultaneous Cell Binding

To demonstrate that the multispecific DB-VHHs are capable to bind simultaneously and bring together at least three different cell types, tumor cells were stained with three different fluorescent cell trackers: HCC-1954 cells were stained with CellTracker Deep Red Dye (Thermo Fisher Scientific, Cat: C34565) diluted 1:20,000 in PBS (50 nM), EBC-1 cells were stained using CellTrace CFSE Cell Proliferation Kit (Thermo Fisher Scientific, Cat: C34554) diluted 1:400,000 in PBS (12.5 nM), MDA-MB-468 and THP-1 cells were stained using CellTracker Orange CMRA Dye (Thermo Fisher Scientific, Cat: C34551) diluted 1:10,000 in PBS (500 nM). Cells were harvested, washed once with PBS and stained at cell density of 1×10^6 cells/ml with the corresponding reagent for 15 min at 37°C in the dark. Cells were centrifuged and excess reagent was blocked by adding cell culture medium (containing 10% fetal bovine serum (FBS)). Next, cells were washed again using PBS + 1% BSA and 1×10^5 cells of each cell line were mixed in a 96-well plate. Parental and recombined DB-VHH constructs were added to the cells at varying concentrations (1–100 nM) and the cells were incubated for 1 h on ice. Next, cells were washed twice and resuspended in 200 µl cold PBS + 1% BSA. Flow cytometry analysis was performed as described above and 10,000 events/sample were recorded and analyzed. As controls, mixed cells without antibody construct were used to determine the "background" cell clustering, and wells with each cell line individually were used for accurate population gating. Flow cytometry cytograms were visualized using FlowJo 10.7.1 software.

Antibody-Mediated Binding of Recombinant IL6R to HCC-1954 and EBC-1 Cell Clusters

HCC-1954 and EBC-1 cells were stained as described above. 1×10^5 cells of each cell line were mixed in a 96-well plate and recombinant human IL6R ECD-His Tag (Sino Biological, Cat: 10398-H08H) was added at a 100 nM concentration. DB-VHHs were mixed at 1–100 nM concentrations and the cells were incubated for 1 h on ice. Afterward, the cells were washed twice with PBS + 1% BSA and were incubated with PE Anti-6x His tag detection antibody (Abcam, Cat: ab72467) diluted 1:20 in PBS + 1% BSA for an additional 1 h on ice. Cells were washed again twice with PBS + 1% BSA, resuspended in 200 µl PBS + 1% BSA and analyzed by flow cytometry as described above.

NK cell-mediated Tumor Cell Lysis

NK cell-mediated cytotoxicity assay was performed as described previously.[28] Blood was drawn at Merck KGaA's medical office, in accordance with Merck internal guidelines and the Declaration of Helsinki. In brief, whole blood samples of healthy human donors were used for isolation of PBMCs by density gradient centrifugation. NK cells were isolated using EasySep Human NK Isolation Kit (Stemcell Technologies, Cat: 17955) and were incubated overnight in complete medium (AIM V) supplemented with 100 U/ml recombinant human IL-2 (R&D Systems, Cat: 10453-IL). On the next day, the NK cell density was adjusted to 0.625×10^6 vc/ml with complete medium. Target tumor cells (EBC-1 and SK-BR-3) were stained with CellTracker Deep Red Dye diluted 1:1000 in PBS (1 µM) as described above. 2,500 target cells (20 µl/well) were mixed with 12,500 NK cells (20 µl/well) and 5 µl antibody constructs in a 10-fold dilution row (10^{-7} to 10^{-12} M end concentration) in a 384-well clear bottom microtiter plate (Greiner Bio-One). SYTOX Green Dead Cell Stain (Invitrogen) was added to the assay at 30 nM for dead cell visualization. NK and target cells without addition of antibody construct were used to determine the tumor cell-dependent NK cell activity (basal killing). Target cells incubated alone with the highest antibody concentration were used as a control for antibody-mediated cytotoxicity. Trastuzumab wild-type and CS06 wildtype (with hIgG1 Fc) were used as positive controls for Fcγ receptor-mediated NK cell activation and target cells incubated in the presence of 0.25% TritonX-100 were used for normalization of the killing activity to 100%. Cells were incubated and imaged every 2 h for at least 24 h using Incucyte Live Cell Analysis System (Sartorius). The ratio of double-fluorescent cells (dead tumor cells) to all red-fluorescent cells (target cells) was used as a measure of the NK cell killing activity. The means of two biological replicates were plotted using GraphPad Prism 9.0.0 software and fitted using a "log(agonist) vs. response" nonlinear regression.

A-NKG2D VHH-mediated Binding of DB-VHHs to Primary NK Cells

Primary NK cells were isolated as described above and were stimulated for 24 h with 100 U/ml recombinant human IL-2 (R&D Systems, Cat: 10453-IL) and 10 ng/ml recombinant human IL-15 (R&D Systems, Cat: 247-ILB) in AIM V medium. Cells were counted, pelleted at $300 \times g$ for 8 min, washed twice with PBS + 1% BSA and transferred to a 96-well plate (1×10^5 cells/well). Cells were incubated in the presence of 100 nM DB-VHH constructs for 1 h on ice. Following washing steps, incubation with detection antibody (Alexa Fluor 488 AffiniPure Fab Fragment Goat Anti-Human IgG (H + L) (Jackson ImmunoResearch, Cat: 109–547-003)) and analysis were performed as described above.

Simultaneous Cell Binding of NK and Cancer Cells

Primary NK cells were isolated as described above and were stimulated for 48 h with 100 U/ml recombinant human IL-2 and 10 ng/ml recombinant human IL-15 in AIM V medium. On the day of the assay, HER2-overexpressing HCC-1954 cells

and c-MET-positive EBC-1 cells were stained with DeepRed and CFSE dyes, respectively, as described above. NK cells were pelleted at $300 \times g$ for 8 min and were washed with PBS. Cells were resuspended at a cell density of 1×10^6 cells/ml in PBS and were stained using 500 nM CMRA dye for 15 min in the dark. Cells were pelleted and the cell tracker reagent was blocked by resuspending in full culture medium (RPMI-1640 + 10% FBS). Next, cells were washed with PBS + 1% BSA and 1×10^5 cells of each cell type were mixed in a 96-well plate. After addition of the DB-VHH constructs, the cells were incubated, washed and analyzed as described above.

Molecular Modeling

Homology models of the full length IgGs and VHHs were generated using the antibody modeler tool in the molecular modeling software package moe (Mol Operating Enrion 2020.09: Chemical Computing Group Inc.; 2020). The generation of IgG-VHH constructs were built by adding the $(G_4S)_3$ linker via moe's protein builder between the IgGs C-terminal and VHHs N-terminal residues, followed by a conformational search of the linker via moe's linker modeler. Finally, an energy minimization was performed, treating the linker as flexible and the IgG and VHH domains as rigid bodies. Structure-based surface hydrophobicity and aggregation propensity was based on (1) moe's "area of hydrophibic protein patches" descriptor and (2) Schrodinger's aggscore (10.1002/prot.25594). The MD simulation was carried out for 50 ns with predefined SPC water model using Schrödinger's Desmond (Schrödinger Release 2021–3: Desmond Molecular Dynamics System, D. E. Shaw Research, New York, NY, 2021. Maestro-Desmond Interoperability Tools, Schrödinger, New York, NY, 2021). Visualization of 3D structures and properties was done with PyMOL (The PyMOL Molecular Graphics System, Version 2.0 Schrödinger, LLC.).

Abbreviations

2-MEA	cysteamine hydrochloride
ADCC	antibody-dependent cell-mediated cytotoxicity
BLI	biolayer interferometry
bsAbs	bispecific antibodies
cFAE	controlled Fab arm exchange
CH3	constant domain 3 of antibody heavy chain
c-MET	tyrosine-protein kinase Met
CODV	cross-over dual variable antibody
DART	dual-affinity re-targeting antibody
DB	DuoBody
DEKK	Fc variant with L351D, L368E mutations in one heavy chain and L351K, T366K in the second heavy chain
DVD-Igs	dual variable domain immunoglobulin
EGFR	epidermal growth factor receptor
Fab	antigen-binding fragment
Fc	fragment crystallizable
FcγRIIIa	Fc-gamma receptor IIIa
FDA	US Food and Drug Administration
GSlinker	glycine-serine linker
HER2	human epidermal growth factor receptor 2
HIC	hydrophobic interaction chromatography
IgG	immunoglobulin G
IL6R	interleukin receptor 6

2-MEA	cysteamine hydrochloride
ADCC	antibody-dependent cell-mediated cytotoxicity
BLI	biolayer interferometry
bsAbs	bispecific antibodies
cFAE	controlled Fab arm exchange
CH3	constant domain 3 of antibody heavy chain
c-MET	tyrosine-protein kinase Met
CODV	cross-over dual variable antibody
DART	dual-affinity re-targeting antibody
DB	DuoBody
DEKK	Fc variant with L351D, L368E mutations in one heavy chain and L351K, T366K in the second heavy chain
DVD-Igs	dual variable domain immunoglobulin
EGFR	epidermal growth factor receptor
Fab	antigen-binding fragment
Fc	fragment crystallizable
FcγRIIIa	Fc-gamma receptor IIIa
FDA	US Food and Drug Administration
GSlinker	glycine-serine linker
HER2	human epidermal growth factor receptor 2
HIC	hydrophobic interaction chromatography
IgG	immunoglobulin G
IL6R	interleukin receptor 6
KB	kinetic buffer
KD	equilibrium dissociation constant
LALA	L234A, L235A Fc silencing double mutation
mAbs	monoclonal antibodies
MW	molecular weight
NK	natural killer
NKG2D	natural killer group 2D receptor
PBMCs	peripheral blood mononuclear cells
PG-LALA	L234A, L235A, P329G Fc silencing triple mutation
SEED	strand-exchanged engineered domains
SE-HPLC	size-exclusion high-performance liquid chromatography
Tm	melting temperature
VHH	variable domain of the heavy chain of a heavy chain only antibody
VH	variable domain of the heavy chain
VL	variable domain of the light chain

Acknowledgments

Disclosure statement

Funding

References

1. Charles A, Janeway J, Travers P, Walport M, Shlomchik MJ. Principles of innate and adaptive immunity. In: Immunobiology: the immune system in health and disease. 5th (New York: Garland Science),26–31 .2001.

2. Charles A, Janeway J, Travers P, Walport M, Shlomchik MJ. The destruction of antibody-coated pathogens via Fc receptors. In: Immunobiology: the immune system in health and disease. 5th (New York: Garland Science), 439–48. 2001.

3. Köhler G, Milstein C. Continuous cultures of fused cells secreting antibody of predefined specificity. Nature. 1975;256(5517):495–97. doi:10.1038/256495a0.

4. Zhang C. Hybridoma technology for the generation of monoclonal antibodies. In: Antibody methods and protocols. Methods Mol Biol. 901 Walker, John M . Totowa (NJ): Humana Press; 2012; p. 117–35. DOI:10.1007/978-1-61779-931-0_7.

5. Mullard A. FDA approves 100th monoclonal antibody product. Nat Rev Drug Discov. 2021; [accessed 2021 Sep 2]. doi:10.1038/d41573-021-00079-7.

6. Fan G, Wang Z, Hao M, Li J. Bispecific antibodies and their applications. J Hematol Oncol. 2015;8(1):1–14. doi:10.1186/s13045-015-0227-0.

7. Krah S, Kolmar H, Becker S, Zielonka S. Engineering IgG-Like bispecific antibodies—An overview. Antibodies. 2018;7(3):28. doi:10.3390/antib7030028.

8. Runcie K, Budman DR, John V, Seetharamu N. Bi-specific and tri-specific antibodies- the next big thing in solid tumor therapeutics. Mol Med. 2018;24(1):50. doi:10.1186/s10020-018-0051-4.

9. Brinkmann U, Kontermann RE. The making of bispecific antibodies. mAbs. 2017;9(2):182–212. doi:10.1080/19420862.2016.1268307.

10. Marvin JS, Zhu Z. Recombinant approaches to IgG-like bispecific antibodies. Acta Pharmacol Sin. 2005;26(6):649–58. doi:10.1111/j.1745-7254.2005.00119.x.

11. Klein C, Sustmann C, Thomas M, Stubenrauch K, Croasdale R, Schanzer J, Brinkmann U, Kettenberger H, Regula JT, Schaefer W. Progress in overcoming the chain association issue in bispecific heterodimeric IgG antibodies. MAbs. 2012;4(6):653–63. doi:10.4161/mabs.21379.

12. Merchant AM, Zhu Z, Yuan JQ, Goddard A, Adams CW, Presta LG, Carter P. An efficient route to human bispecific IgG. Nat Biotechnol. 1998;16(7):677–81. doi:10.1038/nbt0798-677.

13. De Nardis C, Hendriks LJA, Poirier E, Arvinte T, Gros P, Bakker ABH, de Kruif J. A new approach for generating bispecific antibodies based on a common light chain format and the stable architecture of human immunoglobulin G1. J Biol Chem. 2017;292(35):14706–17. doi:10.1074/jbc.M117.793497.

14. Davis JH, Aperlo C, Li Y, Kurosawa E, Lan Y, Lo K-M, Huston JS. SEEDbodies: fusion proteins based on strand-exchange engineered domain (SEED) CH3 heterodimers in an Fc analogue platform for asymmetric binders or immunofusions and bispecific antibodies. Protein Eng Des Sel. 2010;23(4):195–202. doi:10.1093/protein/gzp094.

15. Moretti P, Skegro D, Ollier R, Wassmann P, Aebischer C, Laurent T, Schmid-Printz M, Giovannini R, Blein S, Bertschinger M. BEAT® the bispecific challenge: a novel and efficient platform for the expression of bispecific IgGs. BMC Proceedings ; 23-26 June 2013; Lille, France 2013; 7:O9. doi:10.1186/1753-6561-7-S6-O9.

16. Cohen S, Chung S, Spiess C, Lundin V, Stefanich E, Laing ST, Clark V, Brumm J, Zhou Y, Huang C, et al. An integrated approach for characterizing immunogenic responses toward a bispecific antibody. mAbs. 2021;13(1):1944017. doi:10.1080/19420862.2021.1944017.

17. van der N KM, Schuurman J, Losen M, Bleeker WK, Martínez-Martínez P, Vermeulen E, Den Bleker TH, Wiegman L, Vink T, Aarden LA, et al. Anti-Inflammatory activity of human igg4 antibodies by dynamic Fab arm exchange. Science. 2007;317(5844):1554–57. doi:10.1126/science.1144603.

18. Rispens T, Ooijevaar-de Heer P, Bende O, Aalberse RC. Mechanism of immunoglobulin G4 Fab-arm exchange. J Am Chem Soc. 2011;133(26):10302–11. doi:10.1021/ja203638y.

19. Labrijn AF, Meesters JI, de Goeij BECG, van Den Bremer ETJ, Neijssen J, van Kampen MD, Strumane K, Verploegen S, Kundu A, Gramer MJ, et al. Efficient generation of stable bispecific IgG1 by controlled Fab-arm exchange. PNAS. 2013;110(13):5145–50. doi:10.1073/pnas.1220145110.

20. van Den Bremer Etj, LabrijnAF, van Den BoogaardR, PriemP, SchefflerK, MelisJPM, SchuurmanJ, ParrenPWHI, de JongRN, van Den BremerETJ. Cysteine-SILAC Mass Spectrometry

Enabling The Identification And Quantitation Of Scrambled Interchain Disulfide Bonds: Preservation Of Native Heavy-Light Chain Pairing In Bispecific IgGs generated by controlled Fab-arm exchange. Anal Chem. 2017;89(20):10873–82. doi:10.1021/acs.analchem.7b02543.

21. GramerMJ, van Den BremerET, van KampenMD, KunduA, KopfmannP, EtterE, StinehelferD, LongJ, LannomT, NoordergraafEH, etal. Production of stable bispecific IgG1 by controlled Fab-arm exchange. mAbs. 2013;5(6):962–73. doi:10.4161/mabs.26233.

22. FDA grants accelerated approval to amivantamab-vmjw for metastatic non-small cell lung cancer. U.S. Food and Drug Administration. Center for Drug Evaluation and Research. May 202121 .https://www.fda.gov/drugs/resources-information-approved-drugs/fda-grants-accelerated-approval-amivantamab-vmjw-metastatic-non-small-cell-lung-cancer

23. Castoldi R, Schanzer J, Panke C, Jucknischke U, Neubert NJ, Croasdale R, Scheuer W, Auer J, Klein C, Niederfellner G, et al. TetraMabs: simultaneous targeting of four oncogenic receptor tyrosine kinases for tumor growth inhibition in heterogeneous tumor cell populations. Protein Eng Des Sel. 2016;29(10):467–75. doi:10.1093/protein/gzw037.

24. Xu L, Pegu A, Rao E, Doria-Rose N, Beninga J, McKee K, Lord DM, Wei RR, Deng G, Louder M, et al. Trispecific broadly neutralizing HIV antibodies mediate potent SHIV protection in macaques. Science. 2017;358(6359):85–90. doi:10.1126/science.aan8630.

25. Wu L, Seung E, Xu L, Rao E, Lord DM, Wei RR, Cortez-Retamozo V, Ospina B, Posternak V, Ulinski G, et al. Trispecific antibodies enhance the therapeutic efficacy of tumor-directed T cells through T cell receptor co-stimulation. Nat Cancer. 2020;1(1):86–98. doi:10.1038/s43018-019-0004-z.

26. Deshaies RJ. Multispecific drugs herald a new era of biopharmaceutical innovation. Nature. 2020;580(7803):329–38. doi:10.1038/s41586-020-2168-1.

27. Sawant MS, Streu CN, Wu L, Tessier PM. Toward drug-like multispecific antibodies by design. Int J Mol Sci. 2020;21(20):7496. doi:10.3390/ijms21207496.

28. Pekar L, Busch M, Valldorf B, Hinz SC, Toleikis L, Krah S, Zielonka S. Biophysical and biochemical characterization of a VHH-based IgG-like bi- and trispecific antibody platform. mAbs. 2020;12(1):1812210. doi:10.1080/19420862.2020.1812210.

29. Chen X, Zaro J, Shen W-C. Fusion protein linkers: property, design and functionality. Adv Drug Deliv Rev. 2013;65(10):1357–69. doi:10.1016/j.addr.2012.09.039.

30. Carter P, Presta L, Gorman CM, Ridgway JB, Henner D, Wong WL, Rowland AM, Kotts C, Carver ME, Shepard HM. Humanization of an anti-p185HER2 antibody for human cancer therapy. PNAS. 1992;89(10):4285–89. doi:10.1073/pnas.89.10.4285.

31. Sellmann C, Doerner A, Knuehl C, Rasche N, Sood V, Krah S, Rhiel L, Messemer A, Wesolowski J, Schuette M, et al. Balancing selectivity and efficacy of bispecific epidermal growth factor receptor (EGFR) × c-MET antibodies and antibody-drug conjugates. J Biol Chem. 2016;291:25106–19. doi:10.1074/jbc.M116.753491.

32. Schmitz KR, Bagchi A, Roovers RC, van Bergen En Henegouwen Pmp, Ferguson KM, Van bergen en henegouwen PP. Structural evaluation of egfr inhibition mechanisms for nanobodies/VHH Domains. Structure. 2013;21(7):1214–24. doi:10.1016/j.str.2013.05.008.

33. Compernolle V, Descamps BE, F BE. inventors; Ablynx N.V., BE assignee. Nanobody against IL-6R. United States Patent 10,618,964 2020 April 14

34. Baty D, Chames P, Kerfelec B, Termine E. inventors; Aix Marseille Universite, Centre National de la Recherche Scientifique CNRS, Institut National de la Sante et de la Recherche Medicale INSERM, Institut Jean Paoli et Irene Calmettes, assignees. Anti- nkg2d single domain antibodies and uses thereof. United States Patent US20180327499A1 2018 November 15

35. Schlothauer T, Herter S, Koller CF, Grau-Richards S, Steinhart V, Spick C, Kubbies M, Klein C, Umaña P, Mössner E. Novel human IgG1 and IgG4 Fc-engineered antibodies with completely abolished immune effector functions. PEDS. 2016;29(10):457–66. doi:10.1093/protein/gzw040.

36. Zhang N, Liu L, Dumitru CD, Cummings NRH, Cukan M, Jiang Y, Li Y, Li F, Mitchell T, Mallem MR, et al. Glycoengineered Pichia produced anti-HER2 is comparable to trastuzumab in preclinical study. mAbs. 2011;3(3):289–98. doi:10.4161/mabs.3.3.15532.

37. Wu C, Ying H, Bose S, Miller R, Medina L, Santora L, Ghayur T. Molecular construction and optimization of anti-human IL-1α/β dual variable domain immunoglobulin (DVD-IgTM) molecules. mAbs. 2009;1(4):339–47. doi:10.4161/mabs.1.4.8755.

38. Steinmetz A, Vallée F, Beil C, Lange C, Baurin N, Beninga J, Capdevila C, Corvey C, Dupuy A, Ferrari P, et al. CODV-Ig, a universal bispecific tetravalent and multifunctional immunoglobulin format for medical applications. mAbs. 2016;8(5):867–78. doi:10.1080/19420862.2016.1162932.

39. Lutterbach B, Zeng Q, Davis LJ, Hatch H, Hang G, Kohl NE, Gibbs JB, Pan B-S. Lung cancer cell lines harboring MET gene amplification are dependent on Met for growth and survival. Cancer Res. 2007;67(5):2081–88. doi:10.1158/0008-5472.CAN-06-3495.

40. Liu H, Saxena A, Sidhu SS, Wu D. Fc engineering for developing therapeutic bispecific antibodies and novel scaffolds. Front Immunol. 2017. doi:10.3389/fimmu.2017.00038.

41. Labrijn AF, Janmaat ML, Reichert JM, Parren PWHI. Bispecific antibodies: a mechanistic review of the pipeline. Nat Rev Drug Discov. 2019;18(8):585–608. doi:10.1038/s41573-019-0028-1.

42. Labrijn AF, Meesters JI, Priem P, de Jong Rn, van Den Bremer Etj, van Kampen Md, Gerritsen AF, Schuurman J, Parren PWHI, de Jong RN, et al. Controlled Fab-arm exchange for the generation of stable bispecific IgG1. Nat Protoc. 2014;9(10):2450–63. doi:10.1038/nprot.2014.169.

43. Huang S, Segués A, Hulsik DL, Zaiss DM, Sijts AJAM, van Duijnhoven Smj, van Elsas A, van Duijnhoven SMJ. A novel efficient bispecific antibody format, combining a conventional antigen-binding fragment with a single domain antibody, avoids potential heavy-light chain mis-pairing. J Immunol Methods. 2020;483:112811. doi:10.1016/j.jim.2020.112811.

44. Escobar-Cabrera E, Lario P, Baardsnes J, Schrag J, Durocher Y, Dixit S. Asymmetric Fc engineering for bispecific antibodies with reduced effector function. Antibodies. 2017;6(2):7. doi:10.3390/antib6020007.

45. DeFazio-Eli L, Strommen K, Dao-Pick T, Parry G, Goodman L, Winslow J. Quantitative assays for the measurement of HER1-HER2 heterodimerization and phosphorylation in cell lines and breast tumors: applications for diagnostics and targeted drug mechanism of action. Breast Cancer Res. 2011;13(2):R44. doi:10.1186/bcr2866.

46. Wang J, Anderson MG, Oleksijew A, Vaidya KS, Boghaert ER, Tucker L, Zhang Q, Han EK, Palma JP, Naumovski L, et al. ABBV-399, a c-Met antibody–drug conjugate that targets both MET – amplified and c-Met–overexpressing tumors, irrespective of MET pathway dependence. Clin Cancer Res. 2017;23(4):992–1000. doi:10.1158/1078-0432.CCR-16-1568.

47. Cleary KLS, Chan HTC, James S, Glennie MJ, Cragg MS. Antibody distance from the cell membrane regulates antibody effector mechanisms. J Immunol. 2017;198(10):3999–4011. doi:10.4049/jimmunol.1601473.

48. Ellwanger K, Reusch U, Fucek I, Wingert S, Ross T, Müller T, Schniegler-Mattox U, Haneke T, Rajkovic E, Koch J, et al. Redirected optimized cell killing (ROCK®): a highly versatile multispecific fit-for-purpose antibody platform for engaging innate immunity. MAbs. 2019;11(5):899–918. doi:10.1080/19420862.2019.1616506.

49. Huang L, Shah K, Barat B, Lam C-YK, Gorlatov S, Ciccarone V, Tamura J, Moore PA, Diedrich GM. Multispecific, multivalent antibody-based molecules engineered on the DART® and TRIDENTTM platforms. Current Protoc Immunol. 2020;129(1):e95. doi:10.1002/cpim.95.